

---

# Semi-Structured Deep Distributional Regression: Combining Structured Additive Models and Deep Learning

---

David Rügamer<sup>1</sup> Chris Kolb<sup>2</sup> Nadja Klein<sup>2</sup>

## Abstract

Combining additive models and neural networks allows to broaden the scope of statistical regression and extends deep learning-based approaches by interpretable structured additive predictors at the same time. Existing approaches uniting the two modeling approaches are, however, limited to very specific combinations and, more importantly, involve an identifiability issue. As a consequence, interpretability and stable estimation is typically lost. We propose a general framework to combine structured regression models and deep neural networks into a unifying network architecture. To overcome the inherent identifiability issues between different model parts, we construct an orthogonalization cell that projects the deep neural network into the orthogonal complement of the statistical model predictor. This enables proper estimation of structured model parts and thereby interpretability. We demonstrate the framework's efficacy in numerical experiments and illustrate its special merits in benchmarks and real-world applications.

## 1. Introduction

In many applications it is necessary and important to capture uncertainties of predictions. Different approaches exist to model this (aleatoric) uncertainty and estimate predictive distributions; which we refer to as distributional regression (DR). Examples are quantile regression (Koenker, 2005) or structured additive distributional regression (SADR; see, e.g., Rigby & Stasinopoulos, 2005; Klein et al., 2015). SADR explicitly models the distributional parameters of a distribution  $\mathcal{D}$  and thereby allows to learn the whole distribution. The general idea of modeling distributions has been advocated early in the machine and deep learning literature (e.g., density networks as proposed by Bishop, 1994).

<sup>1</sup>LMU Munich <sup>2</sup>HU Berlin. Correspondence to: David Rügamer <david.ruegamer@googlemail.com>.

Among the approaches that directly model predictive distributions, DR can be considered a natural extension of existing statistical regression models. Classical mean regression is used to estimate the expectation  $\mu := \mathbb{E}_{\mathcal{D}}(Y|\nu)$  of a target variable  $Y$  using input features  $\nu$ . The most fundamental mean regression is commonly known as generalized linear model (GLM; Nelder & Wedderburn, 1972), defining the model's hypothesis space as

$$\mu = \mathbb{E}_{\mathcal{D}}(Y|\nu) = h(\nu^\top w)$$

with model weights or coefficients  $w$  and activation or response function  $h$ . As an extension, generalized additive models (GAMs, Wood, 2017) allow for general structured additive predictors

$$\mu = h(\sum_j f_j(\nu))$$

that also estimate non-linear relationships between features and the outcome through generic function space representations  $f_j$ . GLMs and GAMs usually assume only very few and low-dimensional interactions between features  $\nu$  in the additive predictor  $\sum_j f_j(\nu)$ . Due to the additivity and function space assumptions of feature effects this so-called *structured predictor* allows for a straightforward interpretation of the model components. For example, for a GAM with no interactions,

$$\mu = h(\sum_j f_j(\nu_j)),$$

the contribution of each effect  $f_j(\nu_j)$  on  $h^{-1}(\mu)$  can be quantified explicitly by holding all other effects in the additive predictor constant. SADR extends GAMs by combining the idea of DR and structured predictors. SADR thereby relates various, potentially different additive predictors to each distributional parameter of an arbitrary parametric distribution. As for GAMs, the interpretation of feature effects on each of the distributional parameters, e.g., the non-linear effect of one feature on the variance of a normal distribution, are straightforward to interpret. Yet, structured additive models are limited in their application (mainly tabular data) and their hypothesis space (e.g., not allowing higher-order interactions).

In this work we extend SADR to a more flexible approach we call *semi-structured distributional regression*, combining the structured additive predictor with an *unstructured*

model part learned through a deep neural network (DNN). Our goal is a distributional modeling framework that covers classical deep learning (DL) applications, use cases requiring higher-order feature interactions or multimodal learning settings, while still preserving the interpretability of (lower-dimensional parts of) the model. Existing approaches in deep learning that fuse structured predictors for tabular data with other data modalities in a multimodal network are sometimes referred to as *wide and deep neural networks*. Several approaches exist (see, e.g., Cheng et al., 2016; Pölsterl et al., 2020, for two recent applications), but these wide and deep models only focus on mean regression. Our proposal can thus also be seen as an extension of mean regression wide and deep models to distributional wide and deep networks. We term the combination semi-structured as the statistical regression predictor is always structured, but does not necessarily need to be a wide neural network.

### 1.1. Related Work and Problem Formulation

**Related Work** Existing SADR models in statistics (e.g., Klein et al., 2015) assume a simple structured additive predictor. Several authors have described amalgamations of simpler statistical model and a neural network (NN). Sarle (1994) describe the commonalities and differences between statistical models and NNs, De Waal & Du Toit (2011); Brás-Geraldes et al. (2019) consider GAMs when framed as a NN. Agarwal et al. (2020) propose how to learn the non-linear additive functions of GAMs within a NN using separate networks for each feature. Various authors have also proposed a combination of statistical regression and NNs. Tran et al. (2020) permits a regression predictor in the class of GLMs that is based on a DNN, resulting in a Deep GLM. In Umlauf et al. (2018) a single-layer NN is included in a SADR model for a very specific choice of weight and bias generation, but this approach does not allow for more complex or deep network structures. Existing wide and deep neural networks only focus on modeling the distribution mean (e.g., Cheng et al., 2016; Chen et al., 2018) or hazard in survival regression (Pölsterl et al., 2020).

**Problem Formulation** While approaches marrying statistical regression and DL exist, these methods either do not provide aleatoric uncertainty or are limited to special use cases. More importantly, none of the existing approaches that try to combine interpretable regression and DL actually preserve the interpretability. For instance, consider a Deep GLM that fuses a deep neural network  $d$  with inputs  $\nu$  with a GLM predictor using the same features:

$$h^{-1}(\mu) = \nu^\top w + d(\nu) =: \eta.$$

From the universal approximation theorem (Cybenko, 1989) and related literature, it is well known that  $d$  can potentially approximate any continuous function under certain

conditions. Thus, without loss of generality, assume that  $d(\nu) = \nu^\top m + f(\nu)$ , decoupling the learned effect of  $d$  into a linear part  $\nu^\top m$  and some non-linear effect  $f$  of  $\nu$ . We can directly observe that the Deep GLM encompasses an identifiability issue as we can arbitrarily add or remove a linear portion of  $\nu$  from the linear model part in  $\eta$  and in turn remove or add this portion back to the deep part of the model, e.g.:

$$\nu^\top w + d(\nu) = \nu^\top w + \nu^\top m + f(\nu) = \nu^\top m + \tilde{d}(\nu).$$

While not relevant for prediction, this identifiability issue inhibits interpretability of the model. In the Deep GLM example, it is unclear how much of the linear effect the model will be attributed to the structured predictor and how much to the deep model part. This problem becomes even more entangled for more complex structured predictors as commonly used in GAMs or SADR.

### 1.2. Main Contributions

In this paper, we present a novel neural network-based framework for the combination of SADR and (deep) NNs. We address challenges with estimation and tuning of such a network, and in particular, propose a solution to the inherent identifiability issue in this model class. Our solutions to the latter is an orthogonalization cell. This cell permits the joint modeling of the structured model part and the unstructured NN predictor in a unifying, end-to-end trainable network while preserving the interpretability of structured part. On the one hand, this allows to reproduce classical statistical regression models such as SADR within a neural network architecture with similar or even superior estimation performance. On the other hand, due to the generality of the approach, extensions of existing regression approaches can be build in a straightforward fashion. This, e.g., facilitates combining interpretable structured effects of tabular features with a DNN and to therewith learn potential higher-order interactions, or modeling multimodal data use cases in combination with classical statistical approaches.

After introducing semi-structured deep distributional regression and addressing the accompanied identifiability issue in Section 2, we describe implementation details in Section 3. In Section 4 we first examine how to achieve our model's identifiability. Thereafter, we investigate its estimation and prediction performance in comparison with state-of-the-art DR models. We then apply our method to several benchmark data sets in Section 5. Finally, we will use the proposed framework in a multimodal data setting to predict prices of rental apartments in Section 6.

## 2. Semi-Structured Deep Distributional Regression

In this section, we first introduce SADR and define basic notation. We then present the proposed extension and solution to the identifiability issue in this model class.

### 2.1. Distributional Regression and Notation

As briefly introduced before, SADR models aim at estimating arbitrary parametric distributions  $\mathcal{D}(\theta_1, \dots, \theta_K)$  by learning the corresponding distributional parameters  $\theta = (\theta_1, \dots, \theta_K)^\top$ . SADR allows to regress features  $\nu$  on potentially all parameters  $\theta_k$ ,  $k = 1, \dots, K$  of the outcome distribution  $\mathcal{D}$ . In the spirit of GAMs, each of the  $K$  distributional parameters is related to the given features  $\nu$  through a monotonic and differentiable response function

$$\theta_k(\nu) = h_k(\eta_k(\nu)).$$

The predictors  $\eta_k(\nu) \in \mathbb{R}$  specify the relationship between features  $\nu$  and the (transformed) parameters  $h_k^{-1}(\theta_k)$ .  $h_k$  ensures that possible parameter space restrictions on  $\theta_k$  are fulfilled for each  $\theta_k$ , e.g.  $h_k(\cdot) = \exp(\cdot)$  to ensure positivity for a variance parameter.

### 2.2. Semi-Structured Deep Distributional Regression

Our proposed framework advances SADR by extending the additive predictors  $\eta_k$  to include one or more latent representations learned through a DNN. To this end we embed SADR into a NN and learn the distribution by adapting deep probabilistic modeling approaches. We call our approach semi-structured deep distributional regression (SDDR).

**Output Model Structure** In order to implement SADR in a neural network, we define the last layer of the network as a distributional layer that computes the predicted distribution  $\mathcal{D}(\theta(\nu))$  based on the outputs  $\eta_k(\nu)$  of all parameter subnetworks. Given a realization  $y$  of  $Y$ , the model can be trained by defining the loss as the negative log-likelihood (NLL)  $-\log p_{\mathcal{D}}(y|\hat{\theta}(\nu))$  based on the (probability) density function  $p_{\mathcal{D}}$  with estimated parameters  $\hat{\theta}$ . For simplicity, we consider a univariate outcome  $Y$ , but the generalization to multivariate outcomes is possible.

**Network Inputs** The subnetworks for each distributional parameter process the feature vector  $\nu$ . We define  $\nu$  to include structured linear input features  $\mathbf{x} = (x_1, \dots, x_p) \in \mathbb{R}^p$ , structured non-linear input features  $\mathbf{z} = (z_1, \dots, z_r) \in \mathbb{R}^r$ , and features  $\mathbf{u} = (u_1, \dots, u_q)$  that are passed through a DNN. In the following we focus on simple one dimensional features, i.e.,  $\mathbf{u} \in \mathbb{R}^q$ , but input features such as images with multiple dimensions are equally possible.

**Predictor Structure** The structured predictors  $\eta_k$  in SDDR are assumed to be an additive decomposition of a structured linear part  $f_0(\mathbf{x}) = b + \mathbf{x}^\top \mathbf{w}$ , structured non-linear functions  $f_j(z_j)$  and one or more unstructured predictors  $d_j(\mathbf{u})$  constituting latent features learned through DNNs. The inputs for these DNNs can be subsets of the features  $\mathbf{u}$  and can also be (partially) identical to the features  $\mathbf{x}, \mathbf{z}$ . The generic predictor of a SDDR model is given by

$$\eta_k = f_0(\mathbf{x}) + \sum_{j=1}^r f_j(z_j) + \sum_{j=1}^g d_j(\mathbf{u}).$$

Note that we have suppressed the index  $k$  in the functions  $f_j, d_j$  to not overload the notation. We assume that the DNNs can be represented as  $d_j(\mathbf{u}) = \hat{\mathbf{u}}_j^\top \boldsymbol{\gamma}_j$  with latent features  $\hat{\mathbf{u}}_j$  learned in a network trunk and weights  $\boldsymbol{\gamma}_j$  of a network head. The functions  $f_j(\cdot)$  represent penalized smooth non-linear effects of features using a linear combination of  $L_j$  basis functions. A univariate non-linear effect of feature  $z_j$  is, e.g., approximated by  $f_j(z_j) \approx \sum_{l=1}^{L_j} B_{j,l}(z_j) w_{j,l}$ , where  $B_{j,l}(z_j)$  is the  $l$ th basis function (such as regression splines, polynomial bases or B-splines) evaluated at  $z_j$ . Tensor product representations allow for two- or moderate-dimensional non-linear interactions of a subset of  $\mathbf{z}$ . It is also possible to represent discrete spatial information or cluster-specific effects in this way (see, e.g., [Wood, 2017](#)). Structured predictors are easily understandable, yet limited to low-dimensional structures in order to preserve interpretability and tractability of the model.

**Architecture** The network learns effects of  $\mathbf{x}$  and  $\mathbf{z}$  using a single unit hidden layer with linear activation functions and different regularization terms for each input type. The DNN model part(s) processing  $\mathbf{u}$  can be arbitrarily specified to, e.g., incorporate complex feature interactions. To ensure identifiability (see Section 2.3), an orthogonalization cell combines the different types of features, see Figure 1 and its caption for detailed explanations. For unstructured features  $\hat{\mathbf{u}}$  learned in DNNs, a distinction is made between DNNs whose inputs are also part of the structured inputs  $\mathbf{x}, \mathbf{z}$  and DNNs whose inputs solely appear in the unstructured predictor (xor-node in Figure 1). In the latter case, the DNN outputs are directly summed up as a weighted combination with structured predictors (lower path after xor-node in Figure 1) and fed into the distributional layer. The  $\hat{\mathbf{u}}$  from DNNs that also share inputs with  $\mathbf{x}$  or  $\mathbf{z}$ , an orthogonalization operation is applied before adding its outputs  $\tilde{\mathbf{u}}$  as weighted sum to the remaining predictors.

### 2.3. Identifiability

Identifiability is crucial when features overlap in the structured and unstructured model parts. To derive a theoretical concept assuring identifiability, we assume w.l.o.g. that we are only interested in a linear effect of pre-specified structured features and allow for one additional DNN  $d$

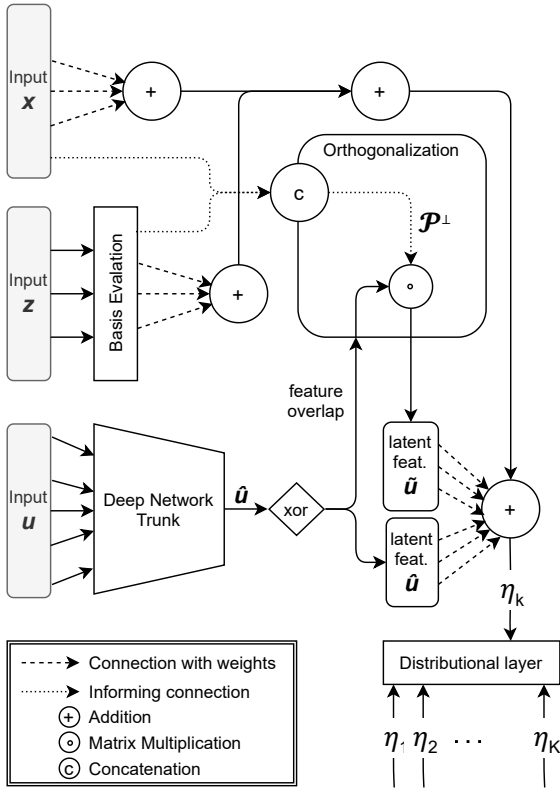


Figure 1. Exemplary SDDR architecture incorporating an orthogonalization cell: Structured linear predictors  $x$  and structured non-linear predictors  $z$  (represented by a basis evaluation) are fed into the cell, concatenated and combined with the deep network using the orthogonalization operation. The solid lines represent the informing connections that either simply combine information or create a projection matrix  $\mathcal{P}^\perp$ , that is multiplied with latent features  $\hat{u}$  to disentangle the structured and unstructured parts. The final additive predictor  $\eta_k$  is created by adding the structured predictors to the (orthogonalized) latent features  $\hat{u}$  multiplied by their weights and is then passed on to a distributional layer.

with arbitrary features in  $\eta_k$  for one distributional parameter  $\theta_k$ . The treatment of the more general case can be found in the Appendix. Let  $(x_1^\top, \dots, x_n^\top)^\top =: \mathbf{X} \in \mathbb{R}^{n \times p}$ ,  $1 \leq p \leq n$ , be the structured feature matrix for  $n \in \mathbb{N}$  observations and  $\mathbf{w} \in \mathbb{R}^p$  the corresponding weights. Further define  $(u_1^\top, \dots, u_n^\top)^\top =: \mathbf{U} \in \mathbb{R}^{n \times q}$  the matrix of features fed into the DNN  $d$ ,  $\hat{\mathbf{U}} \in \mathbb{R}^{n \times s}$ ,  $s \leq n$  the latent unstructured features in the second last layer of  $d$  and let  $\eta_k = (\eta_{1,k}, \dots, \eta_{n,k})^\top \in \mathbb{R}^n$  be the final predictor vector.

If not constrained,  $d$  is able to capture linear effects of any of its features  $\mathbf{U}$ , including those also present in  $\mathbf{X}$ , thus making the attribution of shared effects to either one of the model parts in  $\eta_k$  not identifiable. The following Lemma shows how the orthogonalization induces a meaningful de-

composition of learned effects in  $\eta_k$ .

**Lemma 1. Orthogonalization** Let  $\mathcal{P}_X \in \mathbb{R}^{n \times n}$  the projection matrix for which  $\mathcal{P}_X \mathbf{A}$  is the linear projection of  $\mathbf{A} \in \mathbb{R}^{n \times s}$ ,  $s \leq n$ , onto the column space spanned by the features of  $\mathbf{X}$  and  $\mathcal{P}_X^\perp := \mathbf{I}_n - \mathcal{P}_X$  the projection into the respective orthogonal complement. Then, replacing  $\hat{\mathbf{U}}$  with

$$\tilde{\mathbf{U}} = \mathcal{P}_X^\perp \hat{\mathbf{U}}$$

and multiplying the result with the last layer's weights  $\gamma \in \mathbb{R}^s$ , ensures an identified decomposition of the final predictor

$$\eta_k = \mathbf{X}\mathbf{w} + \tilde{\mathbf{U}}\gamma \quad (1)$$

into a linear part learned from features  $\mathbf{X}$  and a non-linear part learned from  $\tilde{\mathbf{U}}$ .

Lemma 1 can be used to proof the identifiability of structured terms in  $\eta_k$  in the subsequent theorem. The corresponding proofs are given in the supplementary material.

**Theorem 1. Identifiability** Replacing  $\hat{\mathbf{U}}$  with  $\tilde{\mathbf{U}}$  and multiplying the result with the weights  $\gamma$ , ensures identifiability of the structured linear part with respect to the non-linear parts of the DNN in the final predictor (1).

**Remark 1.** If  $x$  and  $z$  overlap in their features, we first use the orthogonalization to ensure identifiability between the structured linear and non-linear part and then combine the two into one joint predictor (not shown in Figure 1). The non-linear part can then be interpreted as the non-linear deviation from the corresponding linear effect.

**Remark 2.** When the DNN and the structured part share  $p$  columns with  $p > n$ ,  $\mathcal{P}_X^\perp$  is equal to a zero matrix  $\mathbf{0}_{n \times n}$ , making  $\tilde{\mathbf{U}}$  de facto irrelevant. In this case the estimated model is equivalent to the defined structured model. We see this edge case rather as a property than a limitation of our framework as the key requirement of the proposed architecture is to provide identifiable structured effects, which in this case is only possible by excluding the unstructured predictor part.

### 3. Implementation Details

Having defined our network structure, we now turn to implementation aspects of SDDR.

#### 3.1. Penalization, Optimization and Tuning

It is believed that neural networks hold an implicit regularization behaviour due to gradient-based optimization (see, e.g., Arora et al., 2019). However, in most of our experiments we observe rather coarse estimated non-linear effects

or even convergence difficulties when not penalizing structured non-linear effects. We therefore allow for additional penalization of non-linear structured effects by regularizing the corresponding weights with tunable smoothing parameter  $\lambda_j$  for each structured non-linear term  $f_j, j \in \{1, \dots, r\}$  and defining matching penalty matrices  $S_j \in \mathbb{R}^{L_j \times L_j}$  (see, e.g., [Wood, 2017](#)). Optimization of the model is done by minimizing the corresponding NLL of  $\mathcal{D}$

$$-\log p_{\mathcal{D}}(y|\hat{\theta}(\nu)) + \sum_{j \in \Lambda} \lambda_j \mathbf{w}_j^\top S_j \mathbf{w}_j$$

with  $\Lambda$  denoting the set of weights that are penalized using an  $L_2$ -penalty or pre-specified quadratic penalty such as those implied by the structured non-linear effects.

**Tuning** Tuning a large number of smooth terms, potentially in combination with DL model parts, is a challenging task. Non-linear structured additive models alone require a sophisticated estimation procedure, often based on second order information and full batch training. This gets even more complicated in semi-structured models. We foster easy training by defining the smoothness of each effect in terms of the degrees of freedom ( $df$ ; see, e.g., [Buja et al., 1989](#)) and implement an efficient calculation using the Demmler-Reinsch Orthogonalization (DRO, cf. [Ruppert et al., 2003](#)). The latter can easily be parallelized or sped up using a randomized singular value matrix decomposition ([Erichson et al., 2019](#)). We thereby also allow for meaningful default penalization by setting  $df_j$  to the same value  $df^*$  for all smooth effects  $j$ . At the same time, we ensure enough flexibility by choosing  $df^* = \min_{j \in J} \max df_j$ , i.e., the largest possible degree of freedom that leaves the least flexible smoothing effect unpenalized and regularizes all others to have the same amount of flexibility.

### 3.2. Model Selection

An important aspect is the choice of features to include in the structured linear and non-linear predictors of the model. In contrast to other regression frameworks, a property of neural networks is their capability of learning a large number of parameters. Combined with the orthogonalization from Section 2.3, our framework seamlessly allows for model selection when including all features in all types of predictor parts (i.e.,  $x_1, \dots, x_v$  being equal to  $z_1, \dots, z_r$  and  $u_1, \dots, u_q$  with  $v \equiv r \equiv q$ ) given that the resulting matrix of structured features has rank smaller  $n$ . This can be seen as a variance decomposition approach, where the model separates the linear and non-linear effects (with no interaction) from the remaining deep unstructured effects. In particular, in contrast to other statistical regression frameworks, this approach does not require any expert knowledge.

### 3.3. Bayesian Interpretation

Uncertainty quantification of estimated model weights in SDDR (epistemic uncertainty) can be accounted for through Bayesian inference paradigms. In a Bayesian network version of our framework, all (or a subset) of layers are replaced by Bayesian layers (BL; [Tran et al., 2019](#)) with prior distribution for their respective weights.

**Prior Assumptions** If no prior information is available to the user, uninformative priors can be defined for all weights in the network. Special treatment has to be given to the structured non-linear effects to ensure smooth partial effects. Having defined the penalization of structured non-linear effects  $f_j$ , their respective penalty matrix  $S_j$  can be used as precision matrix for a zero mean Gaussian prior. Depending on the specification of  $f_j$ , it is not uncommon that  $S_j$  is rank deficient. To guarantee computational feasibility in such cases we add proper priors for the null space of  $S_j$ .

**Posterior Estimation** Posterior distributions are complex and not available in closed form. Several different approaches, such as Markov Chain Monte Carlo (MCMC) or variational inference (VI; [Blei et al., 2017](#)) have been popularized as solutions in the literature. The latter has the main advantage to scale well in high-dimensional applications. VI can be incorporated in our framework using *Bayes by Backprop* ([Blundell et al., 2015](#)), which allows for different combinations of priors for layer's weights and variational posterior families with easy interchangeability.

## 4. Numerical Experiments

We conduct two different simulation experiments to assess the goodness-of-fit in terms of the structured effect estimation and the prediction performance. Our first experiment will demonstrate and proof the efficacy of the orthogonalization cell in practice. The second experiment compares the proposed framework against classical statistical regression frameworks to demonstrate that estimating a penalized SADR works equally well in neural networks. Further experiments can be found in the Appendix.

### 4.1. Identifiability and Interpretability

Here we mimic a situation where the practitioner's interest explicitly lies in decomposing certain feature effects into structured linear, structured non-linear and unstructured non-linear parts, for reasons of interpretability. We simulate 20 data sets with  $n = 1500$  observations and  $p = 10$  features  $x_1, \dots, x_{10}$  drawn from a uniform distribution  $\mathcal{U}(-1, 1)$ . For the outcome  $y$  we consider the cases  $y \sim \mathcal{N}(\eta, s^2)$ ,  $s = 0.1, 1, 10$  (Normal),  $y \sim \text{Ber}(\text{sigmoid}(\eta))$  (Bernoulli) and  $y \sim \text{Po}(\exp(\eta))$  (Poisson). The predictor  $\eta$  contains each feature as linear effect, non-linear effect and an interaction

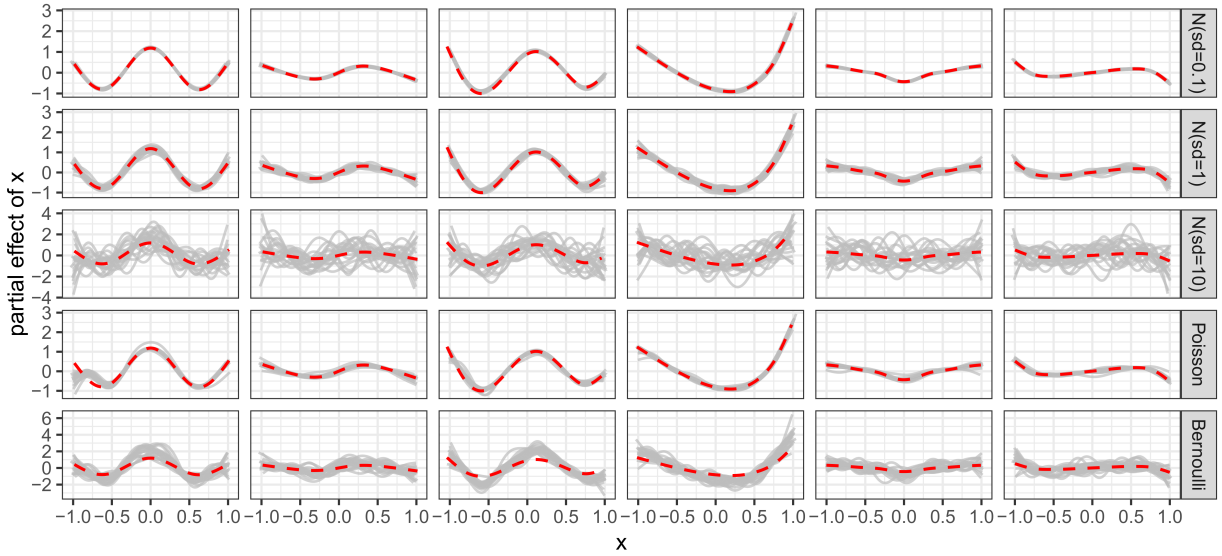


Figure 2. Six selected non-linear partial effects (columns) on the mean of the outcome from the 5 different distributions (rows) with true effect in red and estimated relationships in grey.

with the other 9 features:

$$\eta = \sum_{j=1}^{10} x_j \beta_j + \sum_{j=1}^{10} f_j(x_j) + \prod_{j=1}^{10} x_j.$$

Our framework explicitly models the true linear and non-linear term by separating both effects via orthogonalization and uses a fully connected DNN with two hidden-layers with 32 and 16 hidden units and ReLu activation to account for the interaction. By projecting the output of the second last layer into the orthogonal complement of the structured predictors, we ensure identifiability of the linear and non-linear effects. We do not tune the model but use the DRO approach described in Section 3.1 and a fixed number of epochs.

**Results** Figure 2 visualizes the estimated and true non-linear relationships between selected features and the outcome. Further results can be found in the Supplement A.2. Overall the resulting estimates in Figure 2 demonstrate the capability of the framework to recover the partial non-linear effects and only the simulation using a normal distribution with  $\text{Var}(y) = 100$ , which amounts to a maximum of 4% signal-to-noise ratio (predictor variance divided by noise variance), shows an overfitting behaviour. Most importantly, the results highlight that the DNN, which is also given all 10 features, does not learn the linear or non-linear part of the structured effects and thereby the additive predictor  $\eta$  remains identifiable and interpretable.

## 4.2. Model Comparison

In this simulation we compare the estimation and prediction performance of our framework with three other approaches that implement SADR based on a location, scale and shape (LSS) parameterization. More specifically, we run our approach against a likelihood-based optimization (gamlss; Rigby & Stasinopoulos, 2005), a Bayesian optimization (bamlss Umlauf et al., 2018) and a model-based boosting routine (MBB; Mayr et al., 2012). For three different distributions (normal, gamma, logistic) we investigate a combination of different number of observations  $n \in \{300, 2500\}$  and different number of linear feature effects in the location ( $p \in \{10, 75\}$ ) and 2 linear effects in the scale parameter. In addition to the linear feature effects we add 10 non-linear effects for the location and 2 non-linear effects for the scale.

**Results** Table 1 summarizes the mean log-scores of  $0.25n$  test data points and mean RMSE measuring the average of the deviations between true and estimated structured effects. We observe that our approach (SDDR) often yields the best or second to best estimation and prediction performance, while being robust to more extreme scenarios in which the number of observations is small in comparison to the number of feature effects. In this situation other approaches tend to suffer from convergence problems. We conclude that the estimation of SADR within our neural network framework works equally well to classical statistical approaches, but yields more robust results in high-dimensional settings.

Table 1. Median and median absolute deviation of the mean negative predictive log-scores and mean RMSE values of estimated weights and non-linear point estimates across all settings. The best performing approach with smallest measure each is highlighted in bold.

	n	p	Negative Log-scores				RMSE			
			bamlss	SDDR	gamlss	MBB	bamlss	SDDR	gamlss	MBB
Normal	10	10	<b>1.51</b> (0.68)	1.85 (0.55)	7.08 (8.07)	4.20 (0.47)	0.89 (0.61)	<b>0.37</b> (0.28)	0.59 (0.15)	0.84 (0.22)
		75	> 10e20	<b>2.84</b> (0.94)	> 10e20	10.4 (0.95)	1.05 (1.14)	<b>0.47</b> (0.42)	0.67 (0.26)	1.29 (0.86)
		10	<b>0.55</b> (0.06)	0.96 (0.18)	0.57 (0.08)	3.71 (0.24)	0.50 (0.71)	<b>0.22</b> (0.22)	0.25 (0.34)	0.66 (0.35)
	2500	75	<b>0.64</b> (0.06)	1.11 (0.12)	0.69 (0.07)	8.85 (0.51)	0.48 (0.70)	<b>0.19</b> (0.22)	0.24 (0.32)	1.14 (0.64)
		10	1.15 (0.10)	1.32 (0.31)	<b>1.04</b> (0.09)	1.13 (0.11)	0.13 (0.06)	0.14 (0.04)	<b>0.08</b> (0.02)	0.11 (0.04)
		75	<b>1.50</b> (0.36)	2.34 (0.87)	2.05 (0.99)	1.56 (0.15)	0.15 (0.06)	0.18 (0.07)	<b>0.12</b> (0.05)	0.14 (0.05)
Gamma	10	10	1.01 (0.02)	0.93 (0.03)	<b>0.83</b> (0.02)	0.96 (0.03)	0.19 (0.18)	0.10 (0.04)	<b>0.04</b> (0.03)	0.10 (0.08)
		75	1.01 (0.03)	1.24 (0.05)	<b>0.84</b> (0.03)	1.01 (0.04)	0.19 (0.20)	0.07 (0.03)	<b>0.04</b> (0.02)	0.11 (0.07)
		10	<b>1.44</b> (0.14)	1.75 (0.12)	4.38 (2.84)	3.28 (0.37)	1.69 (0.98)	<b>0.28</b> (0.14)	0.61 (0.18)	0.97 (0.36)
	2500	75	2.55 (0.48)	<b>2.22</b> (0.18)	124 (104)	4.89 (0.26)	1.82 (1.21)	<b>0.26</b> (0.15)	0.66 (0.44)	1.30 (0.84)
		10	1.7 (0.04)	<b>1.15</b> (0.06)	1.15 (0.04)	> 10e20	2.20 (0.82)	<b>0.18</b> (0.15)	0.24 (0.32)	0.73 (0.41)
		75	2.47 (0.36)	<b>1.16</b> (0.08)	1.23 (0.05)	4.71 (0.1)	3.52 (0.97)	<b>0.13</b> (0.13)	0.25 (0.32)	1.19 (0.66)

## 5. Benchmark Studies

In addition to the experiments on synthetic data, we provide a number of benchmarks in several real-world data sets in this section. If not stated otherwise, we report measures as averages and standard deviations (in brackets) over 20 random network initializations. Activation functions for DNNs in SDDR are ReLu for hidden layers and linear for output layers. Additional benchmarks can again be found in the Appendix.

### 5.1. Deep Mixed Models

Tran et al. (2020) use a panel data set with 595 individuals and 4165 observations from Cornwell & Rupert (1988) as an example for fitting deep mixed models by accounting for within subject correlation. Performance is measured in terms of within subject predictions of the log of wage for future time points. We follow their analysis by training the model on the years  $t = 1, \dots, 5$  and predicting the years  $t = 6, 7$ . We use a normal distribution with constant variance and model the mean with the same neural network predictor as done by Tran et al. (2020). However, instead of being part of the DNN, the subject ID is included as a structured random effect  $w_i$  for each individual  $i$ :  $\text{log-wage}_{i,t} \sim \mathcal{N}(b + w_i + d_\mu(\mathbf{x}_i), \exp(d_\sigma(\mathbf{x}_i)))$ , with  $\mathbf{x}_i$  being the 12 features also used in Tran et al. (2020),  $w_i \sim \mathcal{N}(0, \tau^2) \forall i$ , and  $d_\mu, d_\sigma$  two different DNNs.

**Results** Our approach yields an average MSE of 0.04 (0.005) which makes our method competitive to the approach of Tran et al. (2020), who report an MSE of 0.05 for the given data split.

### 5.2. Deep Calibrated Regression

Next, we use the datasets *Diabetes*, *Boston*, *Airfoil*, and *Forest Fire* analyzed by Song et al. (2019) to benchmark our SDDR against the two *post-hoc* calibration methods iso-

tonic regression (IR; Kuleshov et al., 2018) and the GP-Beta model (GPB; Song et al., 2019) with 16 inducing points. The uncalibrated model for the latter two is a Gaussian process regression (GPR) which performed better than ordinary least squares and standard neural networks in Song et al. (2019). The SDDR directly models the parameters of a normal distribution. Here, we only tune the specific structure for the predictors  $\eta_\mu = \mu, \eta_\sigma = \log(\sigma)$ , which consist of structured linear and non-linear effects, as well as a DNN for all features (see the Supplement A.2 for details about each model’s specification). We split the data into 75% for training and 25% for model evaluation, measured by negative log-scores.

**Results** Table 2 suggests that compared to other calibration techniques our method yields more stable results, while permitting interpretable structured effects for features of interest. Even though we did not fine-tune the output distribution, SDDR performs as good as the benchmarks in terms of average negative log-scores.

Table 2. Comparison of neg. log-scores of different methods (columns) on four different UCI repository datasets (rows).

	SDDR	GPR	IR	GPB
Diabetes	<b>5.33</b> (0.00)	5.35 (5.76)	5.71 (2.97)	5.33 (6.24)
Boston	3.07 (0.11)	2.79 (2.05)	3.36 (5.19)	<b>2.70</b> (1.91)
Airfoil	<b>3.11</b> (0.02)	3.17 (6.82)	3.29 (1.86)	3.21 (4.70)
Forest F.	1.75 (0.01)	1.75 (7.09)	<b>1.00</b> (1.94)	2.07 (9.25)

## 6. Application to Multimodal Data

Finally, we present an application of our framework to Airbnb price listing data, available at <http://insideairbnb.com/get-the-data.html>. Various data modalities are included in the data, such as numeric variables for latitude and longitude, integer variables such as number of bedrooms, textual information such as a room description, dates as well as an image of each property (size

Feature(s)	Description	Effect
$x_1, \dots, x_3$	room types	dummy-effect
$x_4, \dots, x_9$	number of beds	dummy-effect
$x_{10}, \dots, x_{13}$	number of bedrooms	dummy-effect
$z_1, \dots, z_4$	accommodates last review (in days) reviews per month review scores	thin-plate splines
$z_{5,1}, z_{5,2}$	longitude, latitude	tensor product spline
$u_1$	images	transfer-learned
$u_2$	description	embedding layer + FC
$u_3$	$x_1, \dots, x_{13}, z_1, \dots, z_4$	FC DNN (16-4-2)

Table 3. Overview of features in the model, their description and how the features are parameterized. FC denotes a fully connected layer with a single unit. The embedding layer is of size 100 for a lookup of 10,000 words with maximum sentence length of 100. The FC DNN architecture consists of 16, 4 and 2 FCs with dropout layers in between and is used to model the interaction of structured features.

$200 \times 200 \times 3$ ). We will focus on apartments in Munich, Germany consisting of 3,504 observations and 73 features. Our goal is to predict the listing price of each apartment in an interpretable structured additive model, while also accounting for the room description and images. For later model inspection we set aside 10% of the data as test set and use 10% of the resulting training data for early stopping. For  $\mathcal{D}$ , we use an inverse gamma distribution, yielding a superior fit compared to other distribution candidates such as the Pareto distribution.  $\mathcal{D}$  is parameterized by its location (mode)  $\mu$  and shape parameter  $\sigma$  with corresponding additive predictors  $\eta_\mu$  and  $\eta_\sigma$ , respectively. To model the distribution's mode of the apartment prices, we define our linear predictor  $\eta_\mu$  as

$$\eta_\mu = b + \sum_{j=1}^{13} x_j w_j + \sum_{j=1}^4 f_j(z_j) + f_5(z_{5,1}, z_{5,2}) + d_{\mu,1}(u_1) + d_{\mu,2}(u_2) + d_{\mu,3}(u_3),$$

with features given in Table 3. For the shape parameter  $\sigma$  we observe a better validation performance when only including a few structured predictors. As for the mode we include the room type as linear (dummy-)effects and a tensor product spline. Further model specifications and test results are given in Appendix.

**Results** Results suggest that structured effects are the main driving factor in our model. As images and descriptions are rather noisy in this data set, this result is not surprising. We observe a strong location effect on the price of apartments. As shown in Figure 3, the more expensive apartments are located in the center of Munich, close to the English garden or in more prestigious areas. Relative to a typical apartment in Munich, the price for an apartment in the central part of Munich can, e.g., be up to 1.4 times

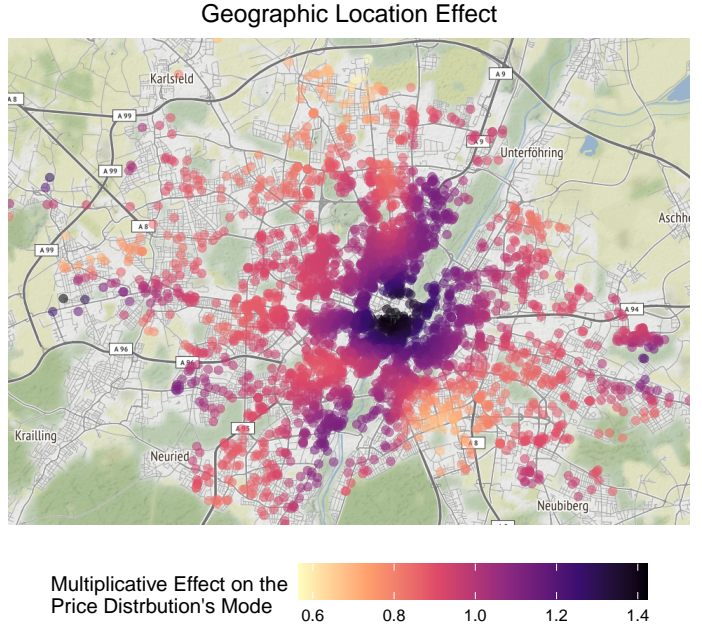


Figure 3. Estimated multiplicative effect (color) of the apartment's geographic location (points on the map) on the mode price value.

more expensive, while a comparable apartment in, e.g., the south might cost only 60% of the average room. The partial effect of the latent feature learned via the images and texts is only slightly correlated with the outcome. The effect of remaining structured non-linear effects are visualized in Figure 4. Here the number of reviews per month has the potential highest impact with an increasing partial multiplicative effect of up to 6 times the mode apartment price.

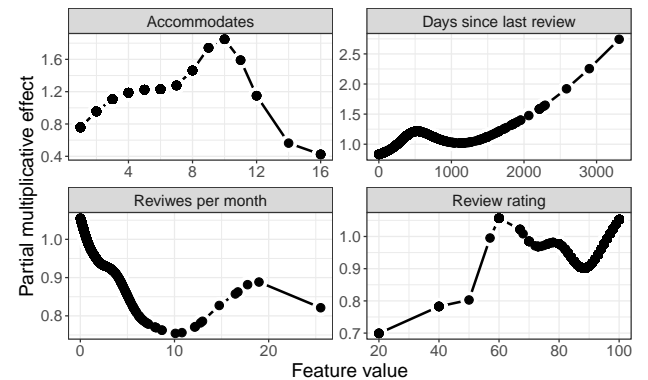


Figure 4. Estimated multiplicative effect (color) of accommodates, days since last review, reviews per month and review rating, on the mean price value.

## 7. Conclusion

In this work we explain why the combination of structured additive models and DNNs is not straightforward. We present a solution that provably allows the identification of structured effects in the presence of more flexible neural networks. We further develop a unified network architecture that combines SADR and DL by embedding the former into a neural network. Using an orthogonalization cell this enables the estimation of (interpretable) structured feature effects next to DNN predictors while ensuring identifiability between the different model parts. Simulations, benchmark and application studies demonstrate the generality of our proposed approach.

### ACKNOWLEDGEMENTS

David Rügamer has been partly funded by the German Federal Ministry of Education and Research (BMBF) under Grant No. 01IS18036A. Nadja Klein acknowledges support through the Emmy Noether grant KL 3037/1-1 of the German research foundation (DFG). The authors of this work take full responsibilities for its content.

## References

Agarwal, R., Frosst, N., Zhang, X., Caruana, R., and Hinton, G. E. Neural Additive Models: Interpretable Machine Learning with Neural Nets. *arXiv preprint arXiv:2004.13912*, 2020.

Arora, S., Cohen, N., Hu, W., and Luo, Y. Implicit regularization in deep matrix factorization. pp. 7411–7422, 2019.

Bishop, C. M. Mixture density networks. 1994.

Blei, D. M., Kucukelbir, A., and McAuliffe, J. D. Variational inference: A review for statisticians. *Journal of the American Statistical Association*, 112(518):859–877, 2017.

Blundell, C., Cornebise, J., Kavukcuoglu, K., and Wierstra, D. Weight uncertainty in neural networks. *Proceedings of the 32nd International Conference on Machine Learning*, 37:1613–1622, 2015.

Brás-Geraldes, C., Papoila, A., and Xufre, P. Generalized additive neural network with flexible parametric link function: model estimation using simulated and real clinical data. *Neural Computing and Applications*, 31(3):719–736, 2019.

Buja, A., Hastie, T., and Tibshirani, R. Linear smoothers and additive models. *The Annals of Statistics*, 17(2):453–510, 1989.

Chen, M. L., Doddi, A., Royer, J., Freschi, L., Schito, M., Ezewudo, M., Kohane, I. S., Beam, A., and Farhat, M. Deep learning predicts tuberculosis drug resistance status from whole-genome sequencing data. *BioRxiv*, pp. 275628, 2018.

Cheng, H.-T., Koc, L., Harmsen, J., Shaked, T., Chandra, T., Aradhye, H., Anderson, G., Corrado, G., Chai, W., Ispir, M., et al. Wide & deep learning for recommender systems. pp. 7–10, 2016.

Cornwell, C. and Rupert, P. Efficient estimation with panel data: An empirical comparison of instrumental variables estimators. *Journal of Applied Econometrics*, 3(2):149–155, 1988.

Cybenko, G. Approximation by superpositions of a sigmoidal function. *Mathematics of control, signals and systems*, 2(4):303–314, 1989.

De Waal, D. A. and Du Toit, J. V. Automation of generalized additive neural networks for predictive data mining. *Applied Artificial Intelligence*, 25(5):380–425, 2011.

Erichson, N. B., Voronin, S., Brunton, S. L., and Kutz, J. N. Randomized matrix decompositions using R. *Journal of Statistical Software*, 89(11), 2019.

Klein, N., Kneib, T., Lang, S., and Sohn, A. Bayesian structured additive distributional regression with an application to regional income inequality in Germany. *Annals of Applied Statistics*, 9(2):1024–1052, 2015.

Koenker, R. *Quantile Regression*, volume Economic Society Monographs. Cambridge University Press, 2005.

Kuleshov, V., Fenner, N., and Ermon, S. Accurate uncertainties for deep learning using calibrated regression. 80: 2796–2804, 2018.

Mayr, A., Fenske, N., Hofner, B., Kneib, T., and Schmid, M. Generalized additive models for location, scale and shape for high-dimensional data - a flexible approach based on boosting. *Journal of the Royal Statistical Society, Series C - Applied Statistics*, 61(3):403–427, 2012.

Nelder, J. A. and Wedderburn, R. W. Generalized linear models. *Journal of the Royal Statistical Society: Series A (General)*, 135(3):370–384, 1972.

Ong, V. M.-H., Nott, D. J., and Smith, M. S. Gaussian variational approximation with a factor covariance structure. *Journal of Computational and Graphical Statistics*, 27(3):465–478, 2018.

Pölsterl, S., Sarasua, I., Gutiérrez-Becker, B., and Wachinger, C. A wide and deep neural network for survival analysis from anatomical shape and tabular clinical

data. *Communications in Computer and Information Science*, pp. 453–464, 2020.

Rigby, R. A. and Stasinopoulos, D. M. Generalized additive models for location, scale and shape. *Journal of the Royal Statistical Society: Series C (Applied Statistics)*, 54(3): 507–554, 2005.

Rodrigues, F. and Pereira, F. C. Beyond expectation: Deep joint mean and quantile regression for spatiotemporal problems. *IEEE Transactions on Neural Networks and Learning Systems*, pp. 1–13, 2020.

Ruppert, D., Wand, M. P., and Carroll, R. J. *Semiparametric regression*. Cambridge University Press, Cambridge and New York, 2003.

Sarle, W. S. Neural networks and statistical models. 1994.

Silverman, B. W. Some aspects of the spline smoothing approach to non-parametric regression curve fitting. *Journal of the Royal Statistical Society: Series B (Methodology)*, 47(1):1–21, 1985.

Song, H., Diethe, T., Kull, M., and Flach, P. Distribution calibration for regression. 97:5897–5906, 2019.

Tran, D., Mike, D., van der Wilk, M., and Hafner, D. Bayesian layers: A module for neural network uncertainty. *33rd Conference on Neural Information Processing System (NeurIPS)*, 2019.

Tran, M.-N., Nguyen, N., Nott, D., and Kohn, R. Bayesian deep net GLM and GLMM. *Journal of Computational and Graphical Statistics*, 29(1):97–113, 2020.

Umlauf, N., Klein, N., and Zeileis, A. Bamlss: Bayesian additive models for location, scale, and shape (and beyond). *Journal of Computational and Graphical Statistics*, 27 (3):612–627, 2018.

Wood, S. N. *Generalized additive models: an introduction with R*. Chapman and Hall/CRC, 2017.

## A. Proofs

**Simplifying assumption** In the main part of the paper we assume only one linear effect and one deep neural network to be present in the model. The given assumptions do not restrict the lemma's and theorem's generality as

1. further non-linear effects can be always represented as linear combination  $Z\delta$  with  $Z = (z_1^\top, \dots, z_r^\top)^\top$  (see, e.g., Wood, 2017). Thus an analogous proof holds when replacing  $\mathbf{X}$  with the composed matrix  $\tilde{\mathbf{X}} := (\mathbf{X}|Z) \in \mathbb{R}^{n \times (p+r)}$  and  $\mathcal{P}_{\tilde{\mathbf{X}}}^\perp$  accordingly with  $\mathcal{P}_{\tilde{\mathbf{X}}}^\perp$ ;
2. further DNN predictors can be orthogonalized individually as the outputs of different DNNs  $d_1, \dots, d_g$  are combined as  $\hat{U}_1\gamma_1 + \dots + \hat{U}_g\gamma_g$ , allowing individual multiplication with  $\mathcal{P}_{\mathbf{X}}$  (or  $\mathcal{P}_{\tilde{\mathbf{X}}}^\perp$ ) from the left;
3. identifiability when mixing several structured effects and several DNNs each with different inputs can be ensured by individually orthogonalizing each DNN output  $\hat{U}_j, j = 1, \dots, g$  with the union of those features, that intersect with any structured effect.

### Proof of Lemma 1 (Orthogonalization)

**Lemma 2. Orthogonalization** Let  $\mathcal{P}_{\mathbf{X}} \in \mathbb{R}^{n \times n}$  the projection matrix for which  $\mathcal{P}_{\mathbf{X}}\mathbf{A}$  is the linear projection of  $\mathbf{A} \in \mathbb{R}^{n \times s}, s \leq n$ , onto the column space spanned by the features of  $\mathbf{X}$  and  $\mathcal{P}_{\mathbf{X}}^\perp := \mathbf{I}_n - \mathcal{P}_{\mathbf{X}}$  the projection into the respective orthogonal complement. Then, replacing  $\hat{U}$  with

$$\tilde{U} = \mathcal{P}_{\mathbf{X}}^\perp \hat{U}$$

and multiplying the result with the last layer's weights  $\gamma \in \mathbb{R}^s$ , ensures an identified decomposition of the final predictor

$$\eta_k = \mathbf{X}\mathbf{w} + \tilde{U}\gamma \quad (2)$$

into a linear part learned from features  $\mathbf{X}$  and a non-linear part learned from features  $\tilde{U}$ .

*Proof.* First decompose the predictor  $\eta_k$  into  $\mathcal{P}_{\mathbf{X}}\eta_k + \mathcal{P}_{\mathbf{X}}^\perp\eta_k$ . Plugging this decomposition into the definition of (2) shows that in the case when a) the true linear effect of  $\mathbf{X}$  is zero, it must hold that  $\eta_k = \mathcal{P}_{\mathbf{X}}^\perp\eta_k$  and thus  $\eta_k = \mathcal{P}_{\mathbf{X}}^\perp(\mathbf{X}\mathbf{w} + \tilde{U}\gamma) = \mathbf{0}_{n \times 1} + \tilde{U}\gamma$ , b) no non-linear effect is present,  $\eta_k = \mathcal{P}_{\mathbf{X}}\eta_k$  and thus  $\eta_k = \mathcal{P}_{\mathbf{X}}(\mathbf{X}\mathbf{w} + \mathcal{P}_{\mathbf{X}}\mathcal{P}_{\mathbf{X}}^\perp\tilde{U}\gamma) = \mathbf{X}\mathbf{w} + \mathbf{0}_{n \times 1}$  and c) both effect types are present multiplying both sides of (2) with either  $\mathcal{P}_{\mathbf{X}}$  or  $\mathcal{P}_{\mathbf{X}}^\perp$  yields the desired property.  $\square$

### Proof of Theorem 1 (Identifiability)

**Theorem 2. Identifiability** Replacing  $\hat{U}$  with  $\tilde{U}$  and multiplying the result with the weights  $\gamma$ , ensures identifiability of the structured linear part with respect to the non-linear parts of the DNN in the final predictor (2).

*Proof.* Assume there exists an identifiability issue of linear effects of  $\mathbf{X}$ , i.e.,  $\exists \xi : \mathcal{P}_{\mathbf{X}}\eta_k = (\mathbf{X}\mathbf{w} - \xi) + \xi$  with  $\mathcal{P}_{\mathbf{X}}\tilde{U}\gamma =: \xi \neq \mathbf{0}_{n \times 1}$ . However, from the decomposition in Lemma 1 it directly follows that  $\xi \equiv \mathbf{0}_{n \times 1}$ .  $\square$

## B. Supplementary Material

Figure 5 visualizes the orthogonalization from a view point of the DNN. The orthogonalization, informed by the structured predictor, is applied to the penultimate layer of the DNN. The resulting orthogonalized outputs are passed on to a single neuron that calculates the weighted sum and passes the result to the distribution parameter.

### B.1. Orthogonalization

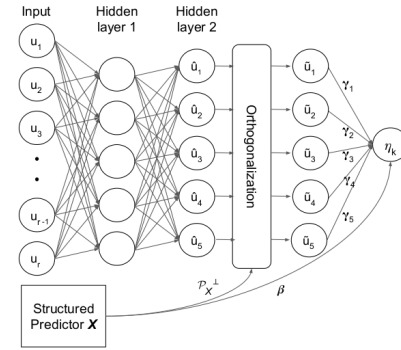


Figure 5. Visualization of the orthogonalization operation: Latent features  $z$  learned in a neural network with two hidden layers are orthogonalized by the defined structured network part before being added to form transformed distribution parameter.

### B.2. Further Results

#### B.2.1. IDENTIFIABILITY AND INTERPRETABILITY

The root mean squared error (RMSE) for the linear effects over different effect sizes ranging from 0.2 to 2 are 0.0145, 0.1725 and 1.2734 for the normal distributions, 0.0394 for the Poisson distribution and 0.6904 for the Bernoulli distribution, which are reasonable small relative to the effect sizes.

#### B.2.2. EPISTEMIC UNCERTAINTY

### B.3. Epistemic Uncertainty

The final simulation has two main purposes. First, we want to compare the estimation performance of our framework when specified with and without BL using the MSE. Second, we investigate 90%-credible intervals using BL for smooth terms to assess the validity of inference statements drawn from the estimated variational posterior distribution. Specif-

ically, we report the point-wise coverage rates and their power measured by the point-wise coverage at zero. We use a homoscedastic normal distribution with  $n = 5000$  observations and either include 1, 3 or 5 structured non-linear predictors  $f_1, \dots, f_5$  that are penalized using  $df^* = 4$ . We also investigate the model fits when using an additional 1 hidden layer neural network with 16 hidden units and / or using a Bayesian version of the network.

**Results:** Results suggest that neither the number of non-linear functions nor the inclusion of a DNN has a notable influence on the performance. Table 4 compares the mean squared deviation between estimated and true curves as well as the coverage and power of corresponding intervals. Simulations with variational layers show slightly better estimation performance for the posterior mean curves in comparison to the non-Bayesian smooth estimation. Intervals tend to be conservative for the first two curves but lack coverage for other smooth functions. Further explanations are given in the supplement.

Table 4. Estimation performance using conventional layers (without BL) or variational layers (with BL) and coverage as well as power results for estimated 90%-credible intervals using BL.

$f_j$	MSE			
	without BL	with BL	Coverage	Power
1	0.01 (0.00)	0.01 (0.00)	1.00 (0.00)	0.83 (0.03)
2	0.03 (0.00)	0.03 (0.00)	0.95 (0.03)	0.07 (0.19)
3	0.09 (0.00)	0.05 (0.01)	0.64 (0.06)	0.12 (0.09)
4	0.08 (0.00)	0.05 (0.01)	0.70 (0.09)	0.91 (0.01)
5	0.09 (0.00)	0.09 (0.00)	0.53 (0.03)	0.00 (0.00)

By varying the degrees-of-freedom of the smooths in further experiments, we found that an appropriate penalization is essential for both proper estimation and the properties of resulting posterior credible intervals. Intervals are too conservative for the first two curves but lack coverage for other smooth functions. Power investigations yield diverse results, but as for coverage, values show better performance for curves for which  $df^* = 4$  induces an appropriate smoothing penalty.

### B.3.1. DEEP DISTRIBUTIONAL MODELS

This application illustrates the distributional aspect of our framework. Following Rodrigues & Pereira (2020), we consider the motorcycle dataset from Silverman (1985). In contrast to Rodrigues & Pereira (2020), who present a framework to jointly predict quantiles, our approach models the entire distribution as  $\mathcal{N}(d_\mu(\text{time}), \exp(b + f(\text{time})))$ , yielding predictions for all quantiles in  $(0, 1)$  in one single model.

**Results:** As we model the distribution itself and not the quantiles explicitly, our approach does not suffer from quantile crossings. Using the quantiles 0.1, 0.4, 0.6 and 0.9, the

approach by Rodrigues & Pereira (2020) yields an RMSE of 0.526 (0.003) with an average of 3.050 (0.999) quantile crossings on all test data points. In contrast, our approach does not suffer from quantile crossings and yields an RMSE of 0.536 (0.016). A visualization of the fitted mean with selected quantiles is depicted in Figure A.2.

Figure A.2 visualizes the results for the analysis of the motorcycle data with estimated mean curve and four different quantiles inferred from the estimated distribution.

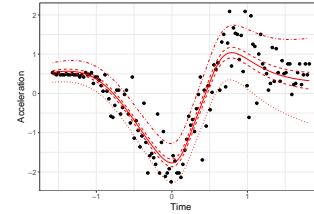


Figure A.2. Acceleration data over time for motorcycle data, with estimated mean (solid line), 40%--, 60%-quantiles (dashed lines) and 10%- as well as 90%-quantiles (dashed-dotted line) in red.

### B.3.2. DEEP CALIBRATED REGRESSION

The SDDR assumes a normal distribution  $\mathcal{N}(\mu, \sigma^2)$  for the output with parameters  $\mu$  and  $\sigma^2$ . We denote their respective DNN predictors by  $d_\mu(\cdot)$  and  $d_\sigma(\cdot)$ , with the number of hidden units in brackets. Specifically for the four data sets, we model  $\mu, \sigma^2$  as  $b_\mu + f(z_3) + d_\mu(4)$ ,  $\exp(b_\sigma + d_\sigma(4))$  (Diabetes);  $b_\mu + \mathbf{x}^\top \mathbf{w} + \sum_{j=1}^{11} f_j(z_j) + d_\mu(32, 16, 4)$ ,  $\exp(b_\sigma + d_\sigma(2))$ , where  $\mathbf{x} = (z_1, \dots, z_J)^\top$  (Boston);  $b_\mu + \sum_{j \in J} f_j(z_j) + d_\mu(16, 4)$ ,  $\exp(b_\sigma + d_\sigma(16, 4))$ , where  $J = \{1, 2, 5\}$  being the indices for three of five available numerical features (Airfoil); and  $b_\mu + d_\mu(16, 4)$ ,  $\exp(b_\sigma + \sum_j w_j)$  with index  $j \in \{1, \dots, 12\}$  for each month (Forest Fire). We use tanh activation functions in the hidden layer(s) and the mentioned number of hidden units for the DNNs.

### B.4. High-dimensional Classification

Ong et al. (2018) aim at predicting various forms of cancer in high-dimensional gene expression data sets (Colon, Leukaemia and Breast cancer). The authors propose VAFC, a Bayesian approach utilising horseshoe priors and VI. We implement SDDR using a Bernoulli distribution and combining a linear model with a small DNN (one or two hidden layers and up to 16 hidden units). The model is applied to all three data sets with training sample sizes of 42, 38 and 38 and test set sizes of 20, 34 and 4, respectively. The number of features is  $p=2000$  (Colon) and  $p=7129$  (Leukaemia, Breast). As an additional comparison, we fit a standard

DNN (sigmoid activation function and binary cross-entropy loss) with the same architecture as for the SDDR approach, but no additional structured predictors.

**Results:** Table 5 compares the average (standard deviation) of the Area under the Receiver Operator Characteristic Curve (AUROC). While all approaches yield an AUROC of one on the Colon cancer data, our SDDR approach is able to outperform the VAFC and standard DNN approach on the other two data sets.

Table 5. Comparison of AUROC on three cancer data sets (first row: Colon cancer; second row: Leukaemia; third row: Breast cancer) for our method, a simple DNN and the VAFC (with different number of factors)

SDDR	DNN	VAFC (4)	VAFC (20)
1.00 (0.00)	1.00 (0.00)	1.00 (0.00)	1.00 (0.00)
<b>0.98</b> (0.02)	0.82 (0.23)	0.91 (0.06)	0.90 (0.07)
<b>1.00</b> (0.00)	<b>1.00</b> (0.00)	0.95 (0.10)	0.84 (0.12)

## B.5. Application

In the application, we first compared different distributions  $\mathcal{D}$  by looking at their log-scores on the training data. The inverse gamma distribution turned out to be the best fit among various choices (Pareto distribution, Gamma distribution, ...). We first estimate a structured model without any deep neural network and use the estimated coefficients as a warm start for the multimodal network. This effectively tackles the problem of different learning speeds of the two model parts without the need for a dedicated optimization routine.

Figure A.2 visualizes the partial effect of images on the apartment prices. The estimated coefficients for the struc-

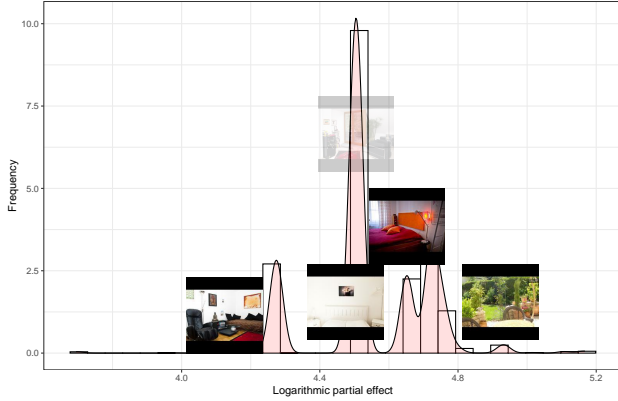


Figure A.2. Estimated partial apartment price based on the latent effect learned from images.

tured linear predictors are given in the following Table 6 with no entries if the effect were not included into the pre-

dictor. The reference in the intercept corresponds to 0 bedrooms and beds (which means either the entry is missing or there is no dedicated bedroom, but instead, e.g., a dormitory) and an entire home or apartment as room type.

	$\eta_\mu$	$\exp(\eta_\sigma)$
Intercept	3.91	0.19
room type = Hotel room	0.33	0.63
room type = Private room	-0.28	0.87
room type = Shared room	-0.59	2.48
bedrooms = 1	0.10	-
bedrooms = 2	0.35	-
bedrooms = 3	0.61	-
bedrooms = 4	0.94	-
beds = 1	0.15	-
beds = 2	0.18	-
beds = 3	0.16	-
beds = 4	0.17	-
beds = 5	0.32	-
beds = 6	0.14	-

Table 6. Partial multiplicative effect of structured linear predictors for the mode ( $\eta_\mu$ ) and shape ( $\eta_\sigma$ )

The effect of the geographic location on the estimated distribution shape is depicted in Figure A.2. Similar to the effect

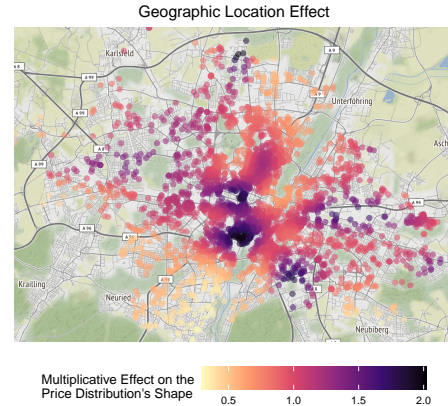


Figure A.2. Estimated multiplicative effect (color) of the apartment's geographic location (points on the map) on the shape of the price value distribution.

on the mode, the shape parameter is larger in the center of Munich, but also in some less prestigious areas. The effect of these locations is yet much more pronounced than the effect on the mode.

To investigate the influence of multimodal data inputs, we further look at the correlation of predicted and true price values on train and test set for different models. We here compare the model with full information as given in the

main article (main) with an only structured effects model (structured), a model with structured effects and only one DNN for  $u_3$  (structured + DNN), a model with structured effects, DNN and text embedding (structured + DNN + texts) as well as two variations where only the images are used (images ResNet-50, images CNN). The results are given in Table 7.

model	cor_train	cor_test
structured	0.68	0.63
structured w/ dnn	0.68	0.64
main	0.68	0.63
structured w/ dnn + embd	0.68	0.64
images CNN	0.70	0.16
images ResNet-50	0.92	0.28

Table 7. Correlations of predicted and true values on train and test set (columns) for the six different models (rows).

Despite heavy regularization, both images-only networks run into overfitting on this rather small data set. This is further exacerbated by the rather uninformative and noisy images. This result supports the use of a structured or semi-structured model.

## C. Details on Computing Environment

Benchmarks and Simulation studies were performed on a linux server with 32 CPUs (Intel(R) Xeon(R) CPU E5-2650 v2 @ 2.60GHz), 64 GB RAM and took between several minutes (Benchmarks, Identifiability Study) to 4 days (Model Comparison Study). The application was performed on a personal computer with 4 CPUs (Intel(R) Core(TM) i7-8665U CPU @ 1.90GHz), 16 GB RAM and took 6.8 hours.